Categorization Of Wear Patterns In Total Hip Arthroplasty HXLPE Bearings Using Machine Learning

Valerio Porrati[1,2,3], Elenora Cabai[1,2,3], Peter Wahl[4,5,6], Deborah J. Hall[1], Joshua J. Jacobs[1], Jonathan A. Gustafson[1], Robin Pourzal[1]
[1]Rush University Medical Center, Chicago, IL, [2]University of Illinois Chicago, Chicago, IL, [3]Politecnico di Milano, Milan, Italy, [4]University of Basel, Allschwil, Switzerland, [5]University of Bern, Bern, Switzerland, [6]Endo-Team, Birshof Hospital, Muenchenstein, Switzerland
Robin_Pourzal@rush.edu

Disclosures: Porrati (N), Cabai (N), Wahl (N), Hall (N), Joshua J. Jacobs (3B-Medtronic Sofamor Danek; 4-Implant Protection; 5-Medtronic Sofamor Danek, Nuvasive, Zimmer), Gustafson (3B- Academic Orthopaedic Consortium (AOC)). Pourzal (2-CeramTec, 5-Stryker, 6-Zimmer-Biomet, Enovis)

INTRODUCTION: Wear of the polyethylene bearing remains one of the main issues in long-term outcomes after total hip arthroplasty (THA). Implant design, materials, surgical positioning, and patient factors drive the tribological impression, resulting in various wear patterns comprised of a combination of wear volume, wear scar shape, and location. Therefore, we designed this study to perform a machine learning-based wear pattern analysis to identify factors driving in vivo wear pattern formation.

METHODS: Eighty-four surgically retrieved THA bearings made from highly-crosslinked polyethylene (HXLPE) implanted for >2 years were available from two manufacturers (Type A – Highcross, Medacta, Type B – Durasul, Zimmer). After examination, 43 were excluded because a) severe removal damage, or b) the in vivo cup orientation was unknown. There were 23 males and 18 female patients, and 33 were Type 1 and 8 were Type 2 HXLPE. The median (min., max.) time in situ, wear volume, and wear rate for the remaining 41 bearings was 10.2 (3, 22) years, 135 (0.7, 575) mm3, and 13 (0.08, 63) mm3/year. Wear maps were generated using an optical coordinate-measuring-machine (RedLux). Two-dimensional (2D) XY-projections of the bearing surfaces, along with the Z-axis representing the deviation from the original sphere, were exported to a .csv file. Prior to export, all THA were normalized to one size, rotated to represent a left side, and scaled within the same coordinate system. Unsupervised learning (k-means and DBSCAN) was used to group implants into clusters based on wear pattern similarity, validating clustering results via silhouette scores and visual inspection. We used Kruskal-Wallis/Mann-Whitney U tests to identify cluster determinants, including wear (volume, rate, and 2D wear vector angle and magnitude), implant design (head size, radial clearance, sphericity), implant positioning (inclination, anteversion), and patient-specific factors (sex, weight, height, age).

RESULTS SECTION: We identified five distinct wear pattern clusters (Fig.1), which were evenly distributed across both bearing types, except cluster 4, which did not contain Type B bearings (Fig.2). We determined significant differences between clusters in wear volume and rate, sphericity of the reconstructed original surface, and the location of the maximum wear as measured by the magnitude and angle of the xy-wear vector. Cluster 4 exhibited the highest wear volume and rate (289.9 mm3, 32.2 mm3/y), followed by 1 (195.9 mm3, 18.7 mm3/y) and 5 (156.3 mm3, 20.1 mm3/y), while clusters 2 (34.5 mm3, 5.6 mm3/y) and 3 (68.7 mm3, 6.9 mm3/y) had the lowest wear volume and rate. The median wear vector angle of clusters 1 and 5 was around 50 degrees within the superior posterior quadrant, and clusters 2-4 exhibited maximum wear between 110 and 140 degrees within the superior-anterior quadrant. Cluster 1 had the lowest wear vector magnitude (0.4), indicating the primary location of maximum wear was closest to the pole. Clusters 1 and 4 exhibited a lower sphericity compared to the others (Cluster 1: 0.007, Cluster 4: 0.007). None of the patient or implant alignment factors were cluster determinants. However, there was a trend (p=0.065) of sex differences between the low wear clusters 2 and 3, with the former being most frequent among female patients. Both clusters exhibited multiple cases with intact machining lines at the pole, which were visible within the light intensity maps (Fig.3). This feature was unique to Type A bearings, but did not warrant its own cluster in our analysis.

DISCUSSION: Our analysis demonstrated distinct differences in wear patterns related to wear volume, wear rate, wear scar location, and initial bearing surface sphericity. The two low-wear clusters included cases that did not exhibit wear at the pole, apparently due to a lack of bearing surface conformity. Owing to our limited sample size, no conclusions could be made on what clinical and surgical factors drive the wear patterns. Another limitation was the lack of patient-specific motion profiles. Our novel technique will yield more definitive findings as the retrieval cohort grows. Ultimately, decoding of wear patterns will provide a better understanding of in vivo wear and inform better pre-clinical testing and implant design.

SIGNIFICANCE/CLINICAL RELEVANCE: Polyethylene wear is still a limiting factor for THA longevity. Additionally, not all types of HXLPE and implant designs perform the same. This study introduces an unbiased machine learning framework to classify distinct in vivo wear patterns of HXLPE bearings. By objectively quantifying wear scar location, magnitude, and geometry, this approach overcomes the limitations of traditional retrieval analyses that rely on subjective categorization. Identifying reproducible wear pattern phenotypes provides a foundation for linking implant performance with patient function, surgical alignment, and implant design in future studies. These findings offer an important step toward developing predictive models that could inform surgical decision-making, implant design optimization, and long-term surveillance of arthroplasty outcomes.

ACKNOWLEDGEMENTS: This study was funded in part by the RMS Foundation.

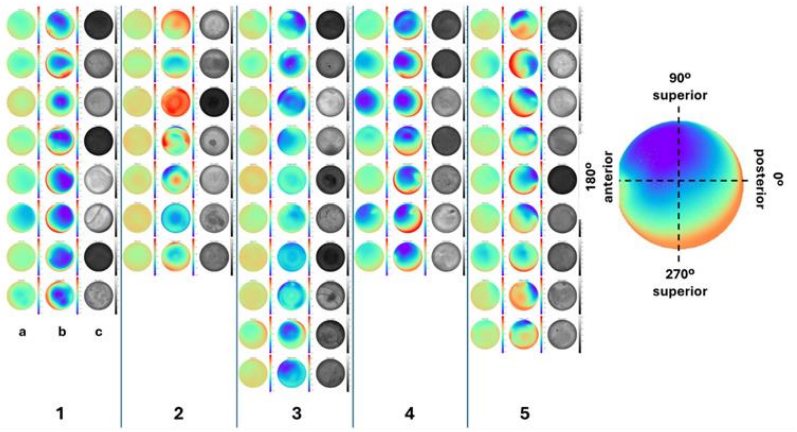

Figure 1 All bearings grouped in 5 clusters: a) columns represent heatmaps on a universal scale, b) columns represent heatmaps on individual scales and the magnitude of the xy-vector, and c) represent light intensity maps.

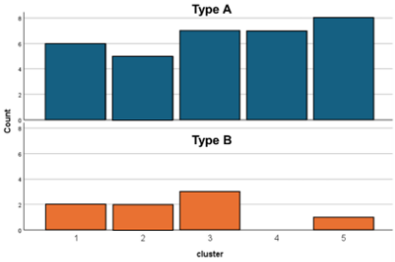

Figure 2 Distribution of clusters for Type A and Type B HXLPE bearings

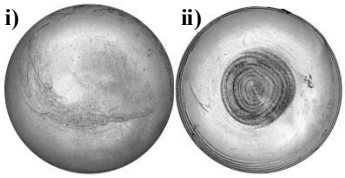

Figure 3 Top-view light intensity images based on optical CMM data showing examples of HXLPE liners with i) wear at the pole, and ii) intact machining lines at the pole. The latter indicates that the femoral head is initially not in contact with the entire HXLPE bearing surface.